International Journal of Pharmaceutics 421 (2011) 176–182

Contents lists available at SciVerse ScienceDirect

International Journal of Pharmaceutics

journal homepage: www.elsevier.com/locate/ijpharm

Evaluating the link between self-assembled mesophase structure and drug release

Stephanie Phan[a], Wye-Khay Fong[a], Nigel Kirby[b], Tracey Hanley[c], Ben J. Boyd[a,*]

[a] Drug Delivery, Disposition and Dynamics, Monash Institute of Pharmaceutical Sciences, Monash University (Parkville Campus), 381 Royal Parade, Parkville, VIC 3052, Australia
[b] SAXS/WAXS Beamline, Australian Synchrotron, Clayton, VIC 3168, Australia
[c] Bragg Institute, Australian Nuclear Science and Technology Organisation, Menai, NSW 2234, Australia

ARTICLE INFO

Article history:
Received 6 May 2011
Received in revised form 16 August 2011
Accepted 19 September 2011
Available online 22 September 2011

Keywords:
Liquid crystal
Cubic phase
Hexagonal phase
Drug release
Diffusion

ABSTRACT

Lipid-based liquid crystalline materials are of increasing interest for use as drug delivery systems. The intricate nanostructure of the reversed bicontinuous cubic (V_2) and inverse hexagonal (H_2) liquid crystal matrices have been shown to provide diffusion controlled release of actives of varying size and polarity. In this study, we extend the understanding of release to other self-assembled phases, the micellar cubic phase (I_2) and inverse micelles (L_2). The systems are comparable as they were all prepared from the one lipid, glyceryl monooleate (GMO), which sequentially forms all four phases with increasing hexadecane (HD) content in excess water. Phase identity was confirmed by small angle X-ray scattering (SAXS). SAXS data indicated that four mesophases were formed with increasing HD content at 25 °C: V_2 phase (*Pn3m* space group) formed at 0–4% (w/w) HD, H_2 phase formed at 4–25% (w/w) HD, I_2 phase (*Fd3m* space group) formed at 25–40% (w/w) HD and finally L_2 phase formed at >40% (w/w) HD. Analogous compositions using phytantriol rather than GMO as the core lipid did not produce the I_2 phase, with only V_2 to H_2 to L_2 transitions being apparent with increasing HD concentration. In order to relate the liquid crystal phase structure to drug release rate, *in vitro* release tests were conducted by incorporating radio-labelled glucose as a model hydrophilic drug into the four GMO-based mesophases. It was found that the drug release followed first-order diffusion kinetics and was fastest from V_2 followed by L_2, H_2, and I_2. Drug release was shown to be significantly faster from bicontinuous cubic phase than the other mesophases, indicating that the state of the water compartments, whether open or closed, has a great influence on the rate of drug release. It is envisioned that liquid crystalline mesophases with slower release characteristics will more likely have potential applications as sustained release drug delivery systems, and hence that the bicontinuous cubic phase is not necessarily the best choice for a sustained release matrix.

1. Introduction

Lipid-based liquid crystalline mesophases of increasing interest across a range of applications, such as in oral and systemic drug delivery (Boyd, 2008; Rizwan et al., 2010), transdermal delivery (Kogan and Garti, 2006) and foods (Mezzenga et al., 2005) due to their highly ordered, thermodynamically stable internal 'mesophase' nanostructure, offering potential as a slow release matrix. These materials are spontaneously formed by adding biocompatible amphiphilic lipids, such as phytantriol and glyceryl monooleate (GMO) to water (Kaasgaard and Drummond, 2006). Studies in the literature have focused on GMO- and phytantriol-based mesophases as they form liquid crystal phases at physiological temperature (Barauskas and Landh, 2003) and are commercially available. The structures of these lipids are illustrated in Fig. 1.

The phase structure formed depends on the packing of lipids within the structure, which in turn depends on the lipid molecular geometry (Israelachvili et al., 1976), (Schwarz and Gompper, 2001) as well as environmental factors such as pH, ionic strength, temperature, pressure and the presence of additives (Fong et al., 2009; Seddon et al., 2000; Shearman et al., 2006; Yaghmur et al., 2010). The mesophases of interest for use as drug delivery systems are illustrated in Fig. 1 and include the viscous reversed bicontinuous cubic (V_2) and inverse hexagonal phases (H_2). The bicontinuous cubic phase consists of two continuous but non-intersecting water channels separated by a lipid bilayer. The inverse hexagonal phase is composed of rod-shaped inverse micelles packed in a hexagonal pattern and in contrast to the bicontinuous cubic phase, in the

* Corresponding author. Tel.: +61 3 99039112; fax: +61 3 99039583.
E-mail address: ben.boyd@monash.edu (B.J. Boyd).

0378-5173/$ – see front matter © 2011 Elsevier B.V. All rights reserved.
doi:10.1016/j.ijpharm.2011.09.022

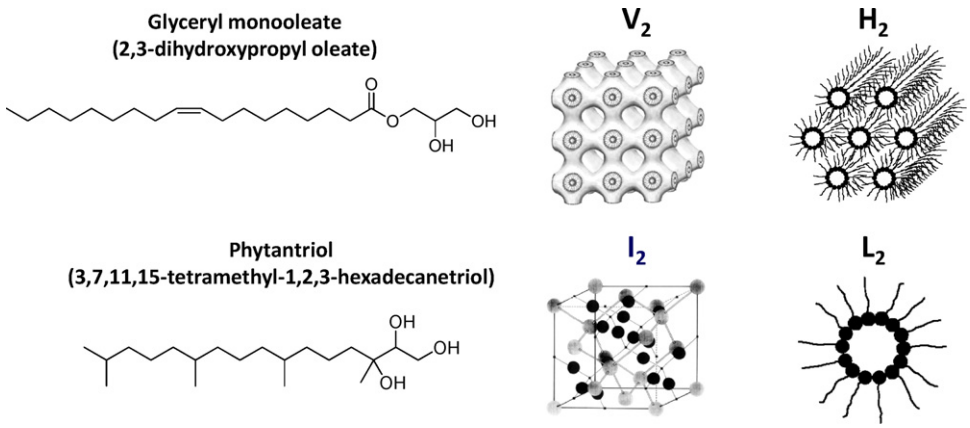

Fig. 1. Chemical structure of glyceryl monooleate and phytantriol (left) and schematics of the four mesophase structures of interest in this study (right).

inverse hexagonal phase the water channels are closed (Kaasgaard and Drummond, 2006). In this study, the inverse micellar cubic phase with *Fd*3*m* space group (I_2) and inverse micelles (L_2) are also of interest. The inverse micellar cubic phase is a closed structure consisting of closely packed inverse micelles of two sizes that are quasi-spherical and arranged in a double diamond network (Luzzati et al., 1992; Pouzot et al., 2007; Yaghmur et al., 2006).

Additives can be incorporated into the liquid crystals to alter the self-assembly of the lipid packing and consequently control the phase structure. The changes in packing can manifest as variations in the lattice dimensions or even complete phase changes (Dong et al., 2006). In excess water, phytantriol and GMO form the bicontinuous cubic phase at ambient temperatures and undergo transition to the inverse hexagonal phase at high temperatures (Briggs et al., 1996; Dong et al., 2006). However with the addition of lipophilic additives, such as vitamin E acetate to phytantriol and oleic acid to GMO, suppression of the V_2 to H_2 phase transition temperature has been observed (Dong et al., 2006; Nakano et al., 2002). The addition of oils has also been reported to transform monolinolein (MLO) cubosomes to hexosomes. Formation of the inverse micellar cubic phase has been demonstrated upon addition of tetradecane (TC) to MLO/water system (Yaghmur et al., 2005, 2006) and addition of limonene to the MLO/water system (Pouzot et al., 2007). Thus it is known that liquid crystalline mesophases can be manipulated via additives to create systems with the desired release characteristics, for example, systems that can provide controlled and sustained release of incorporated molecules (Lee et al., 2009).

Sustained release drug delivery systems aim to maintain drug concentrations in the therapeutic concentration range for a prolonged time frame, to reduce the required frequency of administration, reduce toxicity and minimise side effects. The complex liquid crystal matrix can incorporate molecules of varying size and polarity due to the presence of both lipidic and aqueous domains. For hydrophilic drugs, release from the matrix is controlled by diffusion through the aqueous channels, which is affected by temperature changes and lipid identity, whereas release of lipophilic drugs depends also on the partition coefficient as well as their diffusion through the tortuous water channels (Boyd, 2003; Clogston and Caffrey, 2005). There have been numerous studies characterising the release behaviour from the bicontinuous cubic and inverse hexagonal phases, particularly those formed using GMO (Drummond and Fong, 2000). Lee et al. (2009) showed that bicontinuous cubic and inverse hexagonal phase matrices based on GMO and phytantriol can sustain the release of model hydrophilic drugs like Allura Red, FITC-dextrans and glucose. The group also showed that nanostructure could be changed to alter the rate of drug absorption after oral administration in rats. Release of hydrophilic compounds of dramatically increasing molecular weight from tryptophan to DNA from the GMO-based bicontinuous cubic phase has also been described (Clogston and Caffrey, 2005). Release from mesophases formed from materials other than monoglycerides or phytantriol have also been studied in the literature. Mohammady et al. (2009) have shown complete release of the amino acid arginine from oleoylethanolamide + excess water cubic systems.

In contrast, there have been no studies comparing release from the inverse micellar cubic or inverse micellar mesophases to the other mesophases to enable a clearer understanding of which structures to target in particular applications. In this study, we aim to extend the understanding of drug release to other self-assembled bulk phases, such as I_2 and L_2, compared to V_2 and H_2. Consequently, we sought to identify compositions that would permit study of release from all four mesophases of interest, with minimal changes in composition. Specifically, the effect of addition of hexadecane (HD) to either phytantriol or GMO mesophases was investigated to attempt to generate all four mesophases using one core lipid. This in turn would allow comparison back to existing data. Pseudobinary GMO/phytantriol + HD + excess water phase diagrams were generated and characterised using small angle X-ray scattering (SAXS). Release of a model hydrophilic drug from each mesophase was consequently investigated.

2. Experimental

2.1. Materials

Rylo MG19 Pharma was obtained from Danisco (Grinsted, Denmark) and was used as a commercially available and good model alternative to GMO. The sample consists of 98% monoesters, of which >80% is GMO. Phytantriol (3,7,11,15-tetramethyl hexadecane-1,2,3-triol) was a gift from DSM Nutritional (Singapore). n-Hexadecane (minimum 99%) was obtained from Sigma Aldrich (St. Louis, MO, USA). Lipids were used without further purification. Radio-labelled ^{14}C-glucose (262 mCi/mmol) was sourced from Moravek Biochemicals (Brea, California, USA). D-Glucose was purchased from Sigma Aldrich (St. Louis, MO, USA). Disodium hydrogen orthophosphate, anhydrous was obtained from APS Ajax Finechem (Auburn, NSW, Australia). Potassium dihydrogen orthophosphate and sodium chloride were sourced from BDH AnalR, Merck Pty. Ltd. (Kilsyth, Victoria, Australia). Hydrochloric acid 1 N was purchased from AVS Merck Pty. Ltd. (Kilsyth, Victoria, Australia). Ultima Gold scintillation cocktail was purchased from PerkinElmer (Boston, MA, USA) and 6 mL polypropylene vials for scintillation counting were obtained from Packard Biosciences

(Meriden, CT, USA). Water used was sourced from a Millipore water purification system using a Quantum™ EX Ultrapure Organex cartridge (Millipore, Australia).

2.2. SAXS sample preparation and analysis

Bulk phases of GMO and phytantriol were prepared with increasing HD content. The lipids were weighed in the appropriate amounts into glass HPLC vials and heated to 60 °C until they were flowable and mixed by vortex. Each lipid mixture (0.25 mL) was injected into a 4 mL glass vial containing 2 mL of water and allowed to equilibrate at 25 °C on a tube roller for ≥48 h. Samples were transferred to a stainless steel paste cell (approx 2 mm diameter, 1 mm sample thickness) and sealed with Kapton tape on both sides. The paste cells were then inserted into a thermostatted metal heating block controlled by a waterbath to ±0.1 °C. Sample temperature was established by a thermocouple inserted into a spare sample position in the holder also sealed with Kapton tape. Measurements were performed on the SAXS/WAXS beamline at the Australian Synchrotron. An X-ray beam with a wavelength of 0.83 Å (15 keV) was selected. The 2D SAXS patterns were collected using a Pilatus 1 M detector (170 mm × 170 mm) which was located 966 mm from the sample position. The total q range for the instrument configuration outlined above was $0.02 < q < 1.06$ Å^{-1}. 2D SAXS patterns were collected for 1 s and the computer software SAXS15ID used to acquire and reduce 2D patterns to 1D intensity vs. q profiles. Phase structures were identified by indexing Bragg peaks to known relative spacing ratios and lattice dimensions, a, were calculated using known relationships described by Hyde (Hyde, 2001).

2.3. In vitro release studies

Bulk phases were prepared with 2%, 15%, 35%, 50% HD in GMO to represent the four mesophases investigated (based on the phase diagrams generated using the methods described in Section 2.2), and were composed of 70% (w/w) lipid and 30% (w/w) aqueous solution in PBS at pH 7.4. The 30% (w/w) aqueous composition is slightly below the excess water boundary composition for GMO (Briggs et al., 1996) and phytantriol (Dong et al., 2008) systems to eliminate the potential for a co-existing excess water phase which would result in burst release of drug on immersion of the matrix into the release medium. The aqueous solution contained approximately 10 μCi (10 ng) ^{14}C-glucose per gram of matrix and 170 mg non-radiolabelled glucose per gram of matrix. As described for the phase behaviour studies, the lipids were weighed in the appropriate amounts into glass vials and, after heating to 60 °C until they were flowable, were vortex mixed to ensure complete mixing. The resulting lipidic and aqueous mixture was then thoroughly mixed by heating, vortexing and centrifugation and allowed to equilibrate at 25 °C on a tube roller for ≥48 h.

In vitro release from the four mesophases was then performed in triplicate. PBS pH 7.4 (20 mL in a glass scintillation vial) was used as the release medium. The release medium was prepared by dissolving 2.4 g disodium hydrogen orthophosphate, 0.2 g potassium dihydrogen orthophosphate and 8.0 g sodium chloride per litre MilliQ water, adjusted to pH 7.4 using 0.1 M hydrochloric acid. Approximately 200 mg of bulk liquid crystal phase was loaded into a cylindrical micro beaker with a surface area of 0.6362 cm^2 for drug release, which was then suspended in the release medium. The release medium was stirred magnetically at 100 rpm. The study was performed at 22 °C and ran for five days. For clarity, the experimental set up for the release studies is shown schematically in Supplementary information Fig. S1.

Release medium (100 μL) was removed at predetermined time intervals and replaced with fresh PBS to maintain constant volume. By virtue of its self assembled, thermodynamically stable nature the matrices remained intact in the microbeaker during the experiment, hence there was no requirement to filter the retrieved samples prior to further processing. The sample was combined with 2 mL scintillation cocktail in a 6 mL scintillation vial for scintillation counting on a Tri-Carb 2800TR PerkinElmer Liquid Scintillation Analyser.

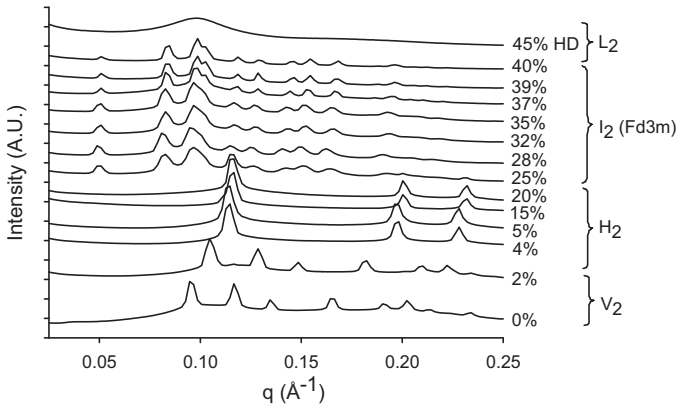

Fig. 2. SAXS profiles for GMO in excess water with increasing hexadecane content at 35 °C. Note that the scattering profiles are displaced on the vertical axis for clarity.

2.3.1. Data treatment and analysis

Inclusion of trace radio-labelled glucose allowed the tracking of release of non-radio-labelled drug molecules, based on the assumption that they behave in an identical manner. The data collected in DPM from scintillation counting for each of the triplicates for each phase was converted to percentage of radiolabelled glucose released against $t^{1/2}$ (h), which was assumed to equal the percentage of total drug released. Where the data showed a linear relationship (in all cases in this study) against $t^{1/2}$, diffusion controlled release is indicated, and the diffusion coefficient for each system was obtained by the use of the previously derived expression (Higuchi, 1967) for diffusion-controlled release from a single sided matrix (1)

$$Q = 2C_0\left(\frac{Dt}{\pi}\right)^{1/2} \quad (1)$$

where Q is the amount of drug released per unit area of matrix, C_0 is the initial amount of drug in unit volume of matrix, D is the diffusion coefficient of the drug in the matrix and t is time.

The mean of the diffusion coefficients for each of the three replicates for each system was taken and the values were analysed by one-way analysis of variance (ANOVA), with significance at a p-value <0.05, to determine the significance between the release rates for the different liquid crystalline phases.

3. Results

3.1. Phase behaviour and characterisation

SAXS measurements on the GMO/HD and phyantriol/HD systems were taken over 20–80 °C. SAXS patterns at defined compositions at varying temperature data points provide information about the phases formed, the phase transition temperatures and the lattice parameters of the systems. Fig. 2 shows intensity vs. q (Å^{-1}) plots obtained from the SAXS diffraction patterns from bulk GMO systems with increasing HD content at 35 °C. The q values of the visible peaks were correlated with Miller indices for known liquid crystalline phases to identify the phase type (Hyde, 2001). The resulting pseudobinary phase diagram for the GMO/HD

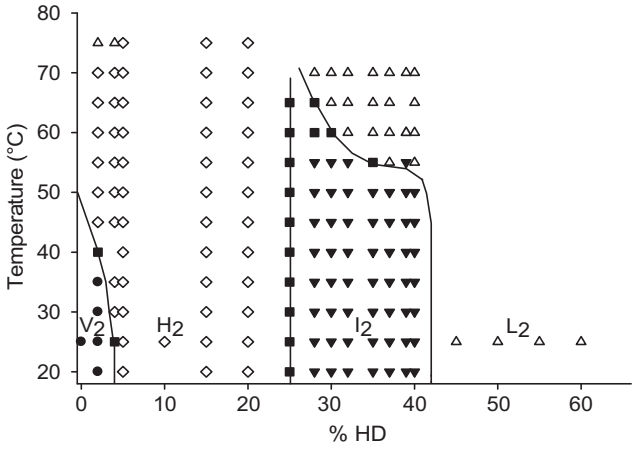

Fig. 3. Partial phase diagram showing the identity and location of each phase and mixed phase regions for the GMO + excess water system with increasing HD concentration and temperature by SAXS. V_2 (●), H_2 (◊), I_2 (▽), L_2 (Δ) and mixed phase regions (■).

system in excess water with increasing temperature is shown in Fig. 3. Four mesophases were formed sequentially with increasing HD content in excess water. In the absence of HD and up to 4% (w/w) HD, the relative positions of the six Bragg peaks are in the ratio $\sqrt{2}:\sqrt{3}:\sqrt{4}:\sqrt{6}:\sqrt{8}:\sqrt{9}$ which are characteristic of the V_2 phase with *Pn*3*m* space group. At 4–25% (w/w) HD, three strong peaks were observed in the ratio $1:\sqrt{3}:\sqrt{4}$, which corresponds to H_2 phase. At compositions between 25% and 40% (w/w) HD, the spacing ratios were $\sqrt{3}:\sqrt{8}:\sqrt{11}:\sqrt{12}:\sqrt{16}:\sqrt{19}$, which is in agreement with I_2 phase with *Fd*3*m* space group. A further increase in HD content >40% (w/w) resulted in one broad peak which is indicative of the L_2 phase. Thus between ambient temperature and 35 °C, which is close to physiological temperature, the phase sequence was V_2, H_2, I_2 and L_2. This enabled us to select four HD concentrations in GMO (2%, 15%, 35%, 50% HD) from which to prepare bulk phases to represent the four mesophases for *in vitro* drug release studies.

The lattice parameter was calculated for each GMO/HD system at 35 °C and shown in Fig. 4. It was found that the I_2 phase has a larger lattice parameter than the other mesophases, 219.7 ± 2.3 Å compared to 89.0 ± 2.5 Å, 56.7 ± 0.5 Å and 67.1 ± 1.5 Å for V_2, H_2 and L_2 respectively. These lattice spacings are consistent with previous reports for GMO-based systems for the V_2, H_2 and L_2 phases (Fong et al., 2009), and with the MLO + tetradecane system in the case of the I_2 phase (Yaghmur et al., 2006).

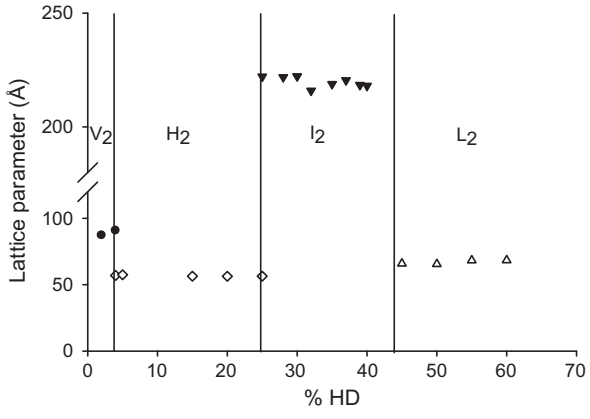

Fig. 4. Variation of lattice parameter (Å) with increasing HD concentration in GMO for the different LC phases observed at 25 °C where V_2 (●), H_2 (◊), I_2 (▽) and L_2 (Δ).

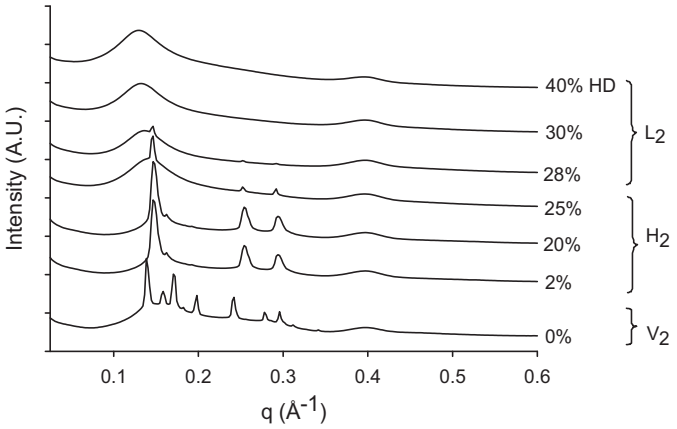

Fig. 5. SAXS profiles for phytantriol in excess water with increasing hexadecane content at 35 °C. Note that the scattering profiles are displaced on the vertical axis for clarity.

The phase behaviour of phytantriol with increasing HD concentration was also investigated, and representative SAXS profiles at 35 °C are shown in Fig. 5. The V_2 phase was expected in the absence of HD, and although this phase dominates the profile, a small peak at $q \sim 0.16\,Å^{-1}$ indicates the presence of a small amount of coexisting H_2 phase, likely due to trace impurities in the batch of phytantriol (Dong et al., 2008). Addition of further HD to just 2% induced a transition completely to the H_2 phase. Transition to the L_2 phase at 28% occurred without encountering the inverse micellar cubic phase seen for the GMO system. The pseudobinary phase diagram for phytantriol/HD in excess water is shown in Fig. 6. The most notable difference when compared to the GMO/HD system in Fig. 3 is that the phases are significantly less thermally stable – the V_2 phase vanishes at <30 °C in the presence of HD, and the H_2 phase melts to the L_2 phase above 65 °C at low HD content, and decreases incrementally with increasing HD up to 25% at which the transition occurs below 20 °C. Because there was no inverse micellar cubic phase region identified in the pseudobinary phase diagram, the phytantriol/HD system was not further investigated.

3.2. In vitro release studies

Fig. 7 illustrates the *in vitro* release of ^{14}C-glucose from the four liquid crystal systems prepared from GMO/HD. There is a significant difference in release rate of ^{14}C-glucose from the systems over

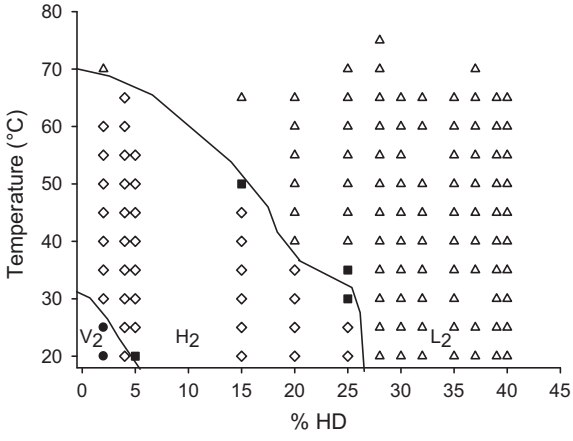

Fig. 6. Partial phase diagram showing the identity and location of each phase and mixed phase regions for the phytantriol + excess water system with increasing HD concentration and temperature by SAXS. V_2 (●), H_2 (◊), I_2 (▽), L_2 (Δ) and mixed phase regions (■).

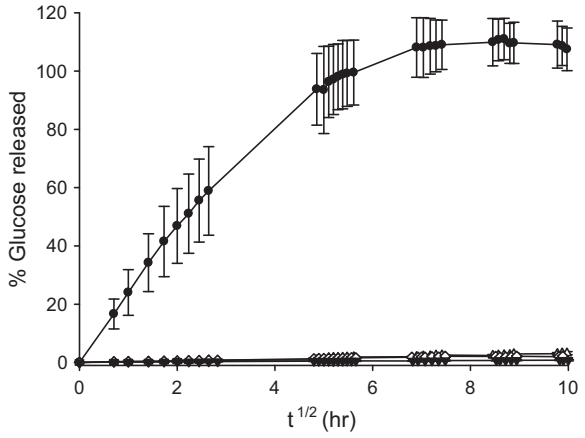

Fig. 7. Model drug (glucose) released (%) from the four mesophases versus square root of time (h) where V_2 (●), L_2 (Δ), H_2 (◊) and I_2 (▽). Data shown as mean ± S.D., $n = 3$.

Table 1
Summary of diffusion coefficients (D) of ^{14}C-glucose from the four mesophases calculated from release data using Eq. (1) (mean ± S.D., $n = 3$). *Indicates significantly different from the other diffusion coefficients ($p < 0.05$).

Mesophase	Diffusion coefficient (D) ($\times 10^{-8}$ cm^2 s^{-1})
V_2	36.3 ± 4.6*
L_2	2.95 ± 1.61
H_2	1.72 ± 0.44
I_2	0.12 ± 0.03

five days. The release from the bicontinuous cubic phase was much more rapid than the other three mesophases. Approximately 100% was released over 50 h, compared to 3%, 2.5% and 0.8% for L_2, H_2 and I_2 respectively. The profiles were approximately linear in all systems except the bicontinuous cubic phase systems, which was seen to plateau after 36 h, as the system started to run out of model drug to release from the matrix. Total recovery of glucose averaged 108% across the $n = 3$ samples for the bicontinuous cubic phase samples, influenced by variability in sampling for total starting concentration and individual release quantitation, but nevertheless close to the anticipated quantitative release based on similar past experiments (Fong et al., 2009; Lee et al., 2009; Negrini and Mezzenga, 2011).

The calculated diffusion coefficients for drug in the matrix over the first 36 h of drug release are presented in Table 1. In line with the release data, the magnitude of the diffusion coefficient ranks in the order $V_2 \gg L_2 > H_2 > I_2$. Diffusion of glucose in the V_2 matrix was shown to be significantly different from the other mesophases by one-way ANOVA test analysis ($p < 0.05$, $n = 3$).

4. Discussion

Liquid crystalline phases are gaining interest for application in sustained release applications. In order to discover, optimise and develop these systems they require the necessary lipid packing behaviour and consequent lyotropic liquid crystalline behaviour to enable control over mesophase structure. The drug release characteristics of the various phase structures then needs to be understood to enable rational selection of formulations with optimal properties. Release behaviour from the inverse micellar cubic (I_2) and inverse micellar (L_2) phases has not received literature attention to date. Further, in order to achieve the required phase behaviour it may be necessary to utilise additives, in the present study hexadecane, and establish the compositional and thermal robustness to changes in the system.

It is well known that phase structure of the liquid crystal mesophases can be altered by modifying lipid packing, by differences in the lipid used and external factors such as pH, ionic strength, temperature, pressure and the presence of additives (Fong et al., 2009; Yaghmur et al., 2010). This behaviour has been manipulated to create stimuli-responsive drug delivery systems, where the most commonly studied systems are those that switch phases in response to changes in temperature and pH. Using GMO and phytantriol systems, Fong et al. (2009) utilised temperature to switch glucose release "off" in the inverse hexagonal phase and "on" in the reversed cubic phase after subcutaneous injection of the matrix into rats. Furthermore, plasmonic nanorods were incorporated into the liquid crystal matrix and near-infrared irradiation used to trigger drug release (Fong et al., 2010). pH-responsive release of the hydrophilic drug phloroglucinol from cubic and hexagonal mesophases has been investigated by Negrini and Mezzenga (2011) in MLO and linoleic acid systems. Linoleic acid is deprotonated at neutral pH and becomes protonated when pH becomes acidic, causing the critical parameter to modify lipid packing, resulting in a reversible change from reverse bicontinous cubic to reverse hexagonal phase, with release from the cubic phase being four times faster.

In this study, the phase structure of the binary GMO/water bulk system was modulated by adding increasing percentages of a third component, the oil, hexadecane (HD) to produce four different mesophases, V_2, L_2, H_2 and I_2 in the temperature range 20–55 °C, which encompasses physiological temperature. This is an essential feature if these systems are to be of use in vivo. These four mesophases were also discovered in previous work by Yaghmur et al. (2006) in a MLO/water dispersed system with the addition of the oil, tetradecane (TC). Both GMO/HD and MLO/TC systems undergo the phase progression of V_2, H_2, I_2, L_2 with increasing oil content, thus it was concluded that it is the addition of oil to the systems that alters lipid packing to produce these phase changes. As seen for the MLO/water system, increasing the temperature at constant oil content, or increasing the oil content at constant temperature induces changes in the mean interfacial curvature to be more negative in the GMO/HD system, due to increased amphiphile chain mobility (Pouzot et al., 2007; Yaghmur et al., 2006). In addition, the inverse micellar cubic phase was not observed at low oil contents, and was present at compositions with less oil than the inverse hexagonal phase, consistent with the inverse micellar cubic phase forming a more negative mean interfacial curvature than the inverse hexagonal phase (Seddon, 1990). The first studies of the inverse micellar cubic phase phase with *Fd*3*m* space group were in systems composed of two lipids with differing amphiphilicities and it was believed that the more polar lipid would partition into the larger, less curved inverse micelles and the opposite for the less polar lipid (Seddon et al., 2000). There is however still some controversy over the exact nature of packing of the lipid components in the inverse micellar cubic phase.

The structure of the inverse micellar cubic phase with *Fd*3*m* space group was determined by Mariani et al. (1990) by crystallographic methods and by Seddon et al. (2000) by electron density maps. It has been reported to be a closed structure composed of two different sizes of discrete, quasi-spherical micelles with different interfacial mean curvatures. The unit cell consists of eight larger inverse micelles of symmetry 43 m arranged tetrahedrally on a diamond lattice and 16 smaller inverse micelles of symmetry 3 m tetrahedrally grouped. These micelles have aqueous domains and they are embedded in a continuous three dimensional hydrophobic matrix formed by the hydrocarbon chains (Luzzati et al., 1992; Pouzot et al., 2007; Seddon, 1990; Yaghmur et al., 2006). The inverse micellar cubic phase is believed to have more severe packing constraints than the inverse hexagonal phase due the balance between the need for the hydrocarbon chains to uniformly fill the

hydrophobic space, and the desire to maintain a uniform mean interfacial curvature. Seddon et al. (1996) described the packing frustration by calculating the packing fraction, where the fraction of volume occupied by the spheres for inverse micellar cubic phase was found to be 0.71 compared to the cylinders for inverse hexagonal phase for 0.91. The I_2 phase like V_2, H_2 and L_2 is stable in excess aqueous phase, thus is of relevance to biological systems (Seddon, 1990).

Phytantriol did not form the inverse micellar cubic phase in excess water in the presence of increasing HD content, but instead the phase progression advanced directly from the H_2 phase to the L_2 phase. It is unlikely that the inverse micellar cubic phase occurred between the samples observed, as the SAXS profiles at 25% and 28% HD in Fig. 5 show the coexisting H_2 and L_2 phases at 25% and a very slight hint of residual H_2 phase at 28%, with no evidence for the presence of the I_2 phase being apparent. The reason that the hexadecane can induce the inverse micellar cubic phase for the GMO system and not the phytantriol system is not immediately clear – although both lipids form the bicontinuous cubic phase in excess water at room temperature, the branched chain of the phytantriol (Fig. 1) may not pack as cooperatively with the straight chain alkane oil as might be expected in the case of the straight chain amphiphile GMO. It is possible that a shorter chained oil or branched oil may have more optimal geometric packing characteristics in the presence of phytantriol to induce formation of the inverse micellar cubic phase. We have previously modified the structure of phytantriol–water bicontinuous cubic phase systems to induce the H_2 phase by inclusion of vitamin E acetate to the phytantriol (Dong et al., 2006), however again no inverse micellar cubic phase has been found in that system. Phytantriol does have some attractiveness in terms of chemical stability, and formation of an inverse micellar cubic phase with phytantriol as the core lipid may have merit in the long term for development of products with enhanced stability. Nevertheless, GMO formed all four desired mesophases with increasing HD content, so the aim of this work in conducting a proof of concept study with drug release could proceed.

In order to relate the liquid crystal phase structure to drug release rate, *in vitro* release tests were conducted. Glucose was utilised to represent a model hydrophilic drug which was then incorporated into the four mesophases. We have used glucose in the past for similar studies as it is stable, and importantly is a rapidly absorbed marker of drug release for future in vivo experiments after both oral (Lee et al., 2009) and subcutaneous administration (Fong et al., 2009).

The rate of drug release from liquid crystalline systems depends on diffusion through the matrix (Higuchi, 1967). Diffusion is in turn dependent on both matrix-related factors such as diameter and tortuosity of water channels, and whether they are open channels or closed micellar compartments and on drug-related factors. Rheological and NMR approaches have both been applied to understanding diffusion processes within lyotropic liquid crystalline mesophases (Sagalowicz et al., 2006). Drug-related factors include solubility and partition behaviour, size (and hence diffusivity). Using the highly water soluble glucose eliminates solubility and partition as a factor in drug release enabling only the matrix structural features to modulate the glucose diffusivity compared to that in bulk aqueous solution. Drug release from V_2 and H_2 has been well established and it is known that release from bicontinuous cubic phase with generally larger open water channels is more rapid than H_2 (Boyd et al., 2006; Clogston and Caffrey, 2005; Fong et al., 2009; Lee et al., 2009). In this study, the release kinetics provided a diffusion coefficient for glucose in the bicontinuous cubic phase of $D = 36 \times 10^{-8}\,cm^2\,s^{-1}$, much faster than the inverse hexagonal phase at $D = 1.7 \times 10^{-8}\,cm^2\,s^{-1}$. These values agree very favourably with the aforementioned work by Negrini and Mezzenga (2011) on diffusion of phloroglucinol (also a small hydrophilic drug) in MLO-based bicontinuous cubic and inverse hexagonal mesophases (D (V_2) $= 31 \times 10^{-8}\,cm^2\,s^{-1}$ and D (H_2) $= 2.2 \times 10^{-8}\,cm^2\,s^{-1}$ respectively). The diffusion coefficients differ slightly from those reported for glucose in the phytantriol ± vitamin E acetate V_2 and H_2 systems, which were approximately 70 and $7 \times 10^{-8}\,cm^2\,s^{-1}$ respectively (Lee et al., 2009), which is understandable as they are prepared from very different lipid systems with differing structural dimensions, however the relative difference in magnitude was again consistent with the more rapid release from the bicontinuous cubic phase.

The 'macro' viscosity of the stiff solid-like cubic phase is often mentioned as responsible for the cubic phase's slow release characteristics. However the closed rod-like micellar structure of the H_2 phase, despite its lower viscosity, retards drug release to a significantly greater extent than the V_2 phase. Glucose release was shown to be slow for the L_2 phase, and extremely slow for I_2 phase. These phases have even lower viscosity generally than the H_2 phase, so there is no link between macroviscosity and drug release characteristics in these systems.

The finding that the inverse micellar cubic phase has a larger lattice parameter than the bicontinuous cubic phase is not surprising as it has been previously reported by Seddon that due to the apparent mixed micellar structure of I_2, its lattice parameter, determined by the repeat distance of the unit cell, is approximately 1.6 times that of a comparable V_2 phase with *Pn*3*m* space group (Seddon, 1990). The lattice parameter was slightly larger in the I_2 phase in the MLO/TC dispersions studied by Yaghmur et al. (2006) compared to V_2, H_2 and L_2 phase. Hence it is also apparent that the lattice parameter cannot be used directly to correlate with the drug release behaviour. What can be concluded is that there is a clear grouping of closed micellar type phase structures that promote very slow release behaviour despite their lower viscosity, while the bicontinuous structure offers less opportunity to maintain drug within the matrix reservoir over time (Ljusberg-Wahren, 1996).

It is envisioned that liquid crystalline mesophases with slower release characteristics will have potential applications in sustained drug delivery systems. The results therefore indicate that bicontinuous V_2 cubic phase is actually a poor choice for a sustained release matrix material based on drug release alone and the other mesophases, such as H_2, I_2 and L_2, may be better utilised as sustained release drug depots in pharmaceutical therapies. The I_2 and L_2 phases can also be dispersed as particles retaining the internal mesophase structure. They have been termed micellar cubosomes and emulsified microemulsions by authors including Nakano et al. (2002), Pouzot et al. (2007) and Yaghmur et al. (2006). The slow drug diffusion indicates at least some potential for a particle-based slow release system using these materials, however this aspect will require future studies.

5. Conclusion

In conclusion, it was found that it was possible to manipulate the GMO/water systems by the addition of increasing quantities of the oil, HD, to sequentially form four mesophases; V_2, H_2, I_2 and L_2 at ambient and physiological temperatures. The *in vitro* release characteristics from these mesophases were established for a model hydrophilic drug, and it was observed that the liquid crystalline structure could be used to control the rate of release. Marked differences were observed between the release rate from V_2, which was significantly faster than release from I_2, L_2 and H_2. The results demonstrate that the distinctive phase structure of these self-assembled mesophases is important in determining the release rate, and confirmed the hypothesis that the state of the aqueous channels, whether they are open or closed, principally influences the rate of drug release. In summary, the unique structural and

physicochemical properties of lipid-based liquid crystalline matrices renders them suitable for use as a drug delivery matrix for hydrophilic drugs. Their ability to form mesophases with highly ordered internal structure and slow rate of drug release could offer promising applications such as sustained release drug delivery systems.

Acknowledgements

The authors thank the Australian Institute of Nuclear Science and Engineering for funding in part the SAXS studies in this manuscript under ALNGRA10057.

Appendix A. Supplementary data

Supplementary data associated with this article can be found, in the online version, at doi:10.1016/j.ijpharm.2011.09.022.

References

Barauskas, J., Landh, T., 2003. Phase behavior of the phytantriol/water system. Langmuir 19, 9562–9565.
Boyd, B.J., 2003. Characterisation of drug release from cubosomes using the pressure ultrafiltration method. International Journal of Pharmaceutics 260, 239–247.
Boyd, B.J., 2008. Past and future evolution in colloidal drug delivery systems. Expert Opinion on Drug Delivery 5, 69–85.
Boyd, B.J., Whittaker, D.V., Khoo, S.M., Davey, G., 2006. Lyotropic liquid crystalline phases formed from glycerate surfactants as sustained release drug delivery systems. International Journal of Pharmaceutics 309, 218–226.
Briggs, J., Chung, H., Caffrey, M., 1996. The temperature-composition phase diagram and mesophase structure characterization of the monoolein/water system. Journal De Physique II 6, 723–751.
Clogston, J., Caffrey, M., 2005. Controlling release from the lipidic cubic phase. Amino acids, peptides, proteins and nucleic acids. Journal of Controlled Release 107, 97–111.
Dong, Y., Dong, A., Larson, I., Rappolt, M., Amenitsch, H., Hanley, T., Boyd, B., 2008. Impurities in commercial phytantriol significantly alter its lyotropic liquid crystalline phase behavior. Langmuir 24, 6998–7003.
Dong, Y.D., Larson, I., Hanley, T., Boyd, B.J., 2006. Bulk and dispersed aqueous phase behavior of phytantriol: effect of vitamin E acetate and F127 polymer on liquid crystal nanostructure. Langmuir 22, 9512–9518.
Drummond, C.J., Fong, C., 2000. Surfactant self-assembly objects as novel drug delivery vehicles. Current Opinion in Colloid & Interface Science 4, 449–456.
Fong, W.-K., Hanley, T., Boyd, B.J., 2009. Stimuli responsive liquid crystals provide 'on-demand' drug delivery *in vitro* and in vivo. Journal of Controlled Release 135, 218–226.
Fong, W.K., Hanley, T.L., Thierry, B., Kirby, N., Boyd, B.J., 2010. Plasmonic nanorods provide reversible control over nanostructure of self-assembled drug delivery materials. Langmuir 26, 6136–6139.
Higuchi, W.I., 1967. Diffusional models useful in biopharmaceutics – drug release rate processes. Journal of Pharmaceutical Sciences 56, 315–324.
Hyde, S., 2001. In: Holmberg, K. (Ed.), Handbook of Applied Surface and Colloid Chemistry. John Wiley & Sons, Ltd., pp. 299–332.
Israelachvili, J.N., Mitchell, D.J., Ninham, B.W., 1976. Theory of self-assembly of hydrocarbon amphiphiles into micelles and bilayers. Journal of the Chemical Society – Faraday Transactions II 72, 1525–1568.
Kaasgaard, T., Drummond, C.J., 2006. Ordered 2-D and 3-D nanostructured amphiphile self-assembly materials stable in excess solvent. Physical Chemistry Chemical Physics 8, 4957–4975.
Kogan, A., Garti, N., 2006. Microemulsions as transdermal drug delivery vehicles. Advances in Colloid and Interface Science 123, 369–385.
Lee, K.W.Y., Nguyen, T.-H., Hanley, T., Boyd, B.J., 2009. Nanostructure of liquid crystalline matrix determines *in vitro* sustained release and in vivo oral absorption kinetics for hydrophilic model drugs. International Journal of Pharmaceutics 365, 190–199.
Ljusberg-Wahren, H.E.A., 1996. Dispersion of the cubic liquid crystalline phase – structure, preparation and functionality aspects. Chimica Oggi 14.
Luzzati, V., Vargas, R., Gulik, A., Mariani, P., Seddon, J.M., Rivas, E., 1992. Lipid polymorphism: a correction. The structure of the cubic phase of extinction symbol Fd – consists of two types of disjointed reverse micelles embedded in a three-dimensional hydrocarbon matrix. Biochemistry 31, 279–285.
Mariani, P., Rivas, E., Luzzati, V., Delacroix, H., 1990. Polymorphism of a lipid extract from pseudomonas-fluorescens – structure-analysis of a hexagonal phase and of a novel cubic phase of ectinction symbol Fd. Biochemistry 29, 6799–6810.
Mezzenga, R., Schurtenberger, P., Burbidge, A., Michel, M., 2005. Understanding foods as soft materials. Nature Materials 4, 729–740.
Mohammady, S.Z., Pouzot, M., Mezzenga, R., 2009. Oleoylethanolamide-based lyotropic liquid crystals as vehicles for delivery of amino acids in aqueous environment. Biophysical Journal 96, 1537–1546.
Nakano, M., Teshigawara, T., Sugita, A., Leesajakul, W., Taniguchi, A., Kamo, T., Matsuoka, H., Handa, T., 2002. Dispersions of liquid crystalline phases of the monoolein/oleic acid/pluronic F127 system. Langmuir 18, 9283–9288.
Negrini, R., Mezzenga, R., 2011. pH-responsive lyotropic liquid crystals for controlled drug delivery. Langmuir 27, 5296–5303.
Pouzot, M., Mezzenga, R., Leser, M., Sagalowicz, L., Guillot, S., Glatter, O., 2007. Structural and rheological investigation of *Fd*3*m* inverse micellar cubic phases. Langmuir 23, 9618–9628.
Rizwan, S.B., Boyd, B.J., Rades, T., Hook, S., 2010. Bicontinuous cubic liquid crystals as sustained delivery systems for peptides and proteins. Expert Opinion on Drug Delivery 7, 1133–1144.
Sagalowicz, L., Mezzenga, R., Leser, M.E., 2006. Investigating reversed liquid crystalline mesophases. Current Opinion in Colloid & Interface Science 11, 224–229.
Schwarz, U.S., Gompper, G., 2001. Bending frustration of lipid–water mesophases based on cubic minimal surfaces. Langmuir 17, 2084–2096.
Seddon, J.M., 1990. An inverse face-centered cubic phase formed by diacylglycerol–phosphatidylcholine mixtures. Biochemistry 29, 7997–8002.
Seddon, J.M., Robins, J., Gulik-Krzywicki, T., Delacroix, H., 2000. Inverse micellar phases of phospholipids and glycolipids. Physical Chemistry Chemical Physics 2, 4485–4493.
Seddon, J.M., Zeb, N., Templer, R.H., McElhaney, R.N., Mannock, D.A., 1996. An *Fd*3*m* lyotropic cubic phase in a binary glycolipid/water system. Langmuir 12, 5250–5253.
Shearman, G.C., Ces, O., Templer, R.H., Seddon, J.M., 2006. Inverse lyotropic phases of lipids and membrane curvature. Journal of Physics – Condensed Matter 18, S1105–S1124.
Yaghmur, A., de Campo, L., Sagalowicz, L., Leser, M.E., Glatter, O., 2005. Emulsified microemulsions and oil-containing liquid crystalline phases. Langmuir 21, 569–577.
Yaghmur, A., de Campo, L., Salentinig, S., Sagalowicz, L., Leser, M.E., Glatter, O., 2006. Oil-loaded monolinolein-based particles with confined inverse discontinuous cubic structure (*Fd*3*m*). Langmuir 22, 517–521.
Yaghmur, A., Kriechbaum, M., Amenitsch, H., Steinhart, M., Laggner, P., Rappolt, M., 2010. Effects of pressure and temperature on the self-assembled fully hydrated nanostructures of monoolein-oil systems. Langmuir 26, 1177–1185.